

Petrogenesis of the Mariquita stock: record of the final pulse of Jurassic to Early Cretaceous arc magmatism in the Northern Andes

Author: Isabel Cardona Gallego

Abstract

Geochemical and magnetic susceptibility variations were used to identify petrogenetic characteristics of the Mariquita stock. This study presents evidence which reveals its juvenile character, high magmatic differentiation, and the consequences it had for the final pulse of Mesozoic arc magmatism in the Central Cordillera of Colombia as well as the possible relationship with the variation of the continental crust thickness during this period. The studied samples exhibit an unimodal distribution of magnetic susceptibility data (Km), ilmenite series affinities, spatial variations of FeO_t , SiO_2 , km , opaque minerals content, and enclaves as indicators of mingling processes. We argue that contrasting features (e.g. juvenile isotopic character, high $SiO_2 > 70$ wt%) on the Mariquita stock are derived from a mixture of depleted mantle and crustal sources. Isotopic trend suggests that this pluton was emplaced near the trench of continental arc apparently during an Early Cretaceous magmatic shutdown.

1. Introduction

Continental arcs are formed due to the subduction of an oceanic slab under a continental crust, where further dehydration of the sediments and the downgoing slab, in this case the oceanic plate will trigger partial melting of the mantle wedge, producing arc-related magmas (Gill, 1981; Stern, 2002). Two classic types of subduction have been proposed to explain the configuration of magmatic arcs. Classification that depends on the strength of mechanical coupling between the subducting slab and the upper plate. Considered as Chilean-type when the two plates are closely coupled implying a compressional stress regime in the arc and back arc regions, the subduction angle is low generating lithospheric thickening of the suprajacent crust (~70 km in thickness) and the subsequent inactivity in the convection of mantle wedge; or Mariana-type when the two plates are virtually decoupled causing a tensional stress regime, the subduction angle is high and develops relatively thin continental crust (~30 km in thickness), furthermore, is associated with a slab rollback process (Uyeda, 1981; Stern, 2002; Ducea et al., 2015).

Continental arc rocks have a large range of silica contents, are calc-alkaline and it contains significant amounts of volatiles (H_2O , CO_2) (Pearce & Peate 1995). Due to continental arc rocks have on average more silicic than basalt, these require additional steps in their magmatic evolution such as prolonged magmatic differentiation processes (Rudnick, 1995),

crustal assimilation, and magma mixing with pre-existing mafic rocks (Hildreth and Moorbath, 1988; Ducea et al., 2015). These processes compose the prolonged history of subduction where variations of the subduction parameters (e.g. subduction dip, convergence angle, degree of plate decoupling, and the amount of fluids released during subduction) affects the volumes of magma and the presence or absence of accompanying vulcanism (Stern, 2002; Gorczyk et al., 2007; Silva and Kay, 2018).

A protracted magmatic activity gives rise to formation of Cordilleran batholiths as the subduction-related arcs of the western margin of the Americas where are Earth's largest sites of intermediate magmatism and they are long lived which means that lived tens to hundreds of million of years and spatially complex (Ducea et al., 2001). However, arc magmatism may be further interrupted by different mechanisms: 1) shallowing of the subducting slab; 2) oblique convergence; 3) change in convergence rate or 4) melt-drained source region (Ducea, 2001; Gorczyk et al., 2007).

A classic example of a continental magmatic arc is located in the Northern Andes including Ecuador and Colombia (Cochrane et al., 2014; Bustamante et al., 2016; Leal-Mejía et al., 2019). Several batholiths comprises a large NNE- trending elongated magmatic bodies as products of this magmatism. (Aspden et al., 1987; Toussaint, 1995). (Figura 1). They are predominantly metaluminous, calc-alkaline and I-type magmatic rocks (Leal-Mejía, 2011; Bustamante et al., 2016; Spikings et al., 2019). Since Jurassic to Early Cretaceous arc magmatism several plutons were installed along the Central Cordillera of Colombia with composition ranging from tonalite to granodiorite (Figure 1) (Cochrane et al., 2014; Bustamante et al., 2016; Zapata et al., 2017; Rodríguez et al., 2017) and intruding Permo-Triassic metamorphic rocks (Vinasco et al., 2006; Villagómez et al., 2011; Bustamante et al., 2017). The recent increasing number of geochemical and geochronological data on this magmatism is focused on unravel its tectono-magmatic evolution, and some aspects of their petrogenesis remains elusive.

Furthermore, Bustamante et al., (2016) propose convergence obliquity since the Middle Jurassic between Farallon Plate and NW margin of South America, what would generate a translation of blocks since south-to-north, so the arc would be in a different position than the Mesozoic. Ultimately, a subduction erosion model was proposed to explain the magmatism in southern Colombia, in which there would be a west to east migration of the magmatism (Rodríguez et al., 2017). Identifying the petrogenetic processes that influenced in the granitoids developed during the final pulse of Jurassic to Early Cretaceous arc magmatism in the Central Cordillera, will allow to clarify about the general tectonic context that dominated the NW margin of South America during this period and the causes of its shut-down.

The Mariquita stock can be considered the last record of arc magmatism in the Late Jurassic-Early Cretaceous of the Central Cordillera with U/Pb crystallization ages spanning from 143 to 129 Ma (Bustamante et al., 2016) and K-Ar dates in biotite of 113 ± 4 Ma (Barrero and Vesga, 1976; Vesga and Barrero, 1978). This stock located in the north of Tolima Department

was named by Barrero and Vesga (1976) has an approximate area of 65 km², and intrudes metamorphic rocks that belongs to the Cajamarca Complex (Figure 2) (Bustamante et al., 2016), generating a contact metamorphism during the Early Cretaceous (Celis et al., 2016). . In addition, compositions of this pluton ranging from granodiorite to tonalite and has high SiO₂>70 wt% indicating magma evolution or differentiation processes but with more juvenile isotopic character ($\epsilon_{\text{Hf}} > 5.0$; Bustamante et al., 2016).

The aim of this study is identify the petrogenetic characteristics of Mariquita stock, analyzing the geochemical information available on whole-rock, isotopic data, and new susceptibility data in order to explore the causes of its juvenile character, high differentiation and the consequences it has for the final pulse of Jurassic to Early Cretaceous arc magmatism in the Northern Andes, in addition to its possible relationship with the thickening or thinning processes of the continental crust in this period.

2. Geological Setting

The Andes in Colombia is divided into the Western, Central and Eastern Cordilleras, which are separated by the Cauca River Valley and Magdalena River Valley respectively that have formed during the Cenozoic (Toussaint and Restrepo, 1994; Villagómez et al., 2011; Spikings et al., 2015). The Western Cordillera is limited on the east the Cauca-Patia fault zone, which is marked by a discontinuous belt of ophiolitic rocks (McCourt and Aspden, 1983) and comprises Cretaceous oceanic terranes that have accreted to the continental margin since the Late Cretaceous and is intruded by numerous Mesozoic granitoids (McCourt, 1984; Toussaint and Restrepo, 1988; Kerr et al., 1997; Villagómez et al., 2011; Villagómez and Spikings., 2013). The Eastern Cordillera include a Proterozoic metamorphic basement composed of Precambrian gneisses, granulites, amphibolites and Ordovician to Silurian granitoids that are covered by Paleozoic transitional siliciclastic and carbonate deposits (Restrepo-Pace et al., 1997; Cordani et al., 2005; Cardona-Molina et al., 2006; Ordóñez-Carmona et al., 2006; Van der Lelij et al., 2016). Also contains Late Triassic to Early Jurassic siliciclastic series covered by an extensive Jurassic to Early Cretaceous transgressive sequence, with extensional structures and the magmatism is represented by limited gabbroic plutons (Vásquez and Altenberger, 2005; Vásquez et al., 2010).

The Central Cordillera consists of Paleozoic metamorphic belt of oceanic and continental character that includes Permian to Triassic I-type magmatic rocks, migmatites, amphibolites and Precambrian remnants (McCourt, 1984; Vinasco et al., 2006; Cochrane et al., 2014; Spikings et al., 2015) that belongs to the Cajamarca Complex (Maya and González, 1995). The Mesozoic magmatic record in the Central Cordillera is characterized by several intrusions of Late Jurassic to Late Cretaceous from tonalite to granodiorite (Aspden et al., 1987; Villagómez et al., 2011; Bustamante et al., 2016) which is related to a continental magmatic arc as product of the Farallon plate subduction under the NW margin of South

America (Aspden et al., 1987; Villagómez et al., 2011; Cochrane et al., 2014). These plutons intrudes the Permian–Triassic rocks, and older metamorphic basement (Figure 1) (Vinasco et al., 2006; Restrepo et al., 2011; Villagómez et al., 2011; Martens et al., 2014).

Mesozoic plutonism in the Southern Central Cordillera in the Upper Magdalena Valley is characterized by plutons such as the Ibagué Batholith that is one of the largest Jurassic plutons of the Central Cordillera and intrudes a pre -Jurassic metamorphic basement. . Other Jurassic plutons as the Altamira, Las Minas, Garzón granites (Bustamante et al., 2016) and Mocoa batholith (Aspden et al., 1987; Zapata et al., 2017) and the Payandé stock which intrudes Late Triassic carbonate rocks (Figure 1.a).

Instead, Early Cretaceous plutons are limited and comprises the Florencia stock and Mariquita stock. Florencia stock intrudes Cajamarca Complex but it also intrudes the dome complex of the Escondido volcano (Figure 1) (Rueda-Guitierrez, 2019). This pluton classify as I-type granite, it has compositions ranging from granodiorite to tonalite, and is composed by albite plagioclase (45-62%), quartz (16-37%), K-feldspar (1,7-13%) and biotite (4-13%) with SiO₂ contents of 61,83, 67,31, and 72,42% wt. Moreover, Florencia stock has crystallization ages spanning from 132 ±2,6 to 129,8±9,7 Ma (Rueda-Guitierrez, 2019). Chondrite-Normalized Rare Earth Element (REE) patterns show a negative Eu anomalie, Light Rare Earth Elements (LREE) enrichment and depleted Rare-Earth Element- Heavy Rare-Earth Elements (MREE-HREE) patterns (Rueda-Guitierrez, 2019).

2.1. The Mariquita stock

Mariquita stock intrudes metamorphic rocks of the Cajamarca Complex and it has an approximate area of 65 km² with compositions ranging from granodiorite to tonalite(Figure 2) (Barrero and Vesga., 1976). This pluton has been covered by Tertiary sedimentary rocks (Barrero and Vesga., 1976) (Figure 2), and is the record of the final pulse of Jurassic to Early Cretaceous arc magmatism in the Northern Andes (Bustamante et al., 2016). In addition, cataclastic processes associated with the Mulatos Fault System have affected igneous and metamorphic rocks of the study zone (Celis et al., 2016).

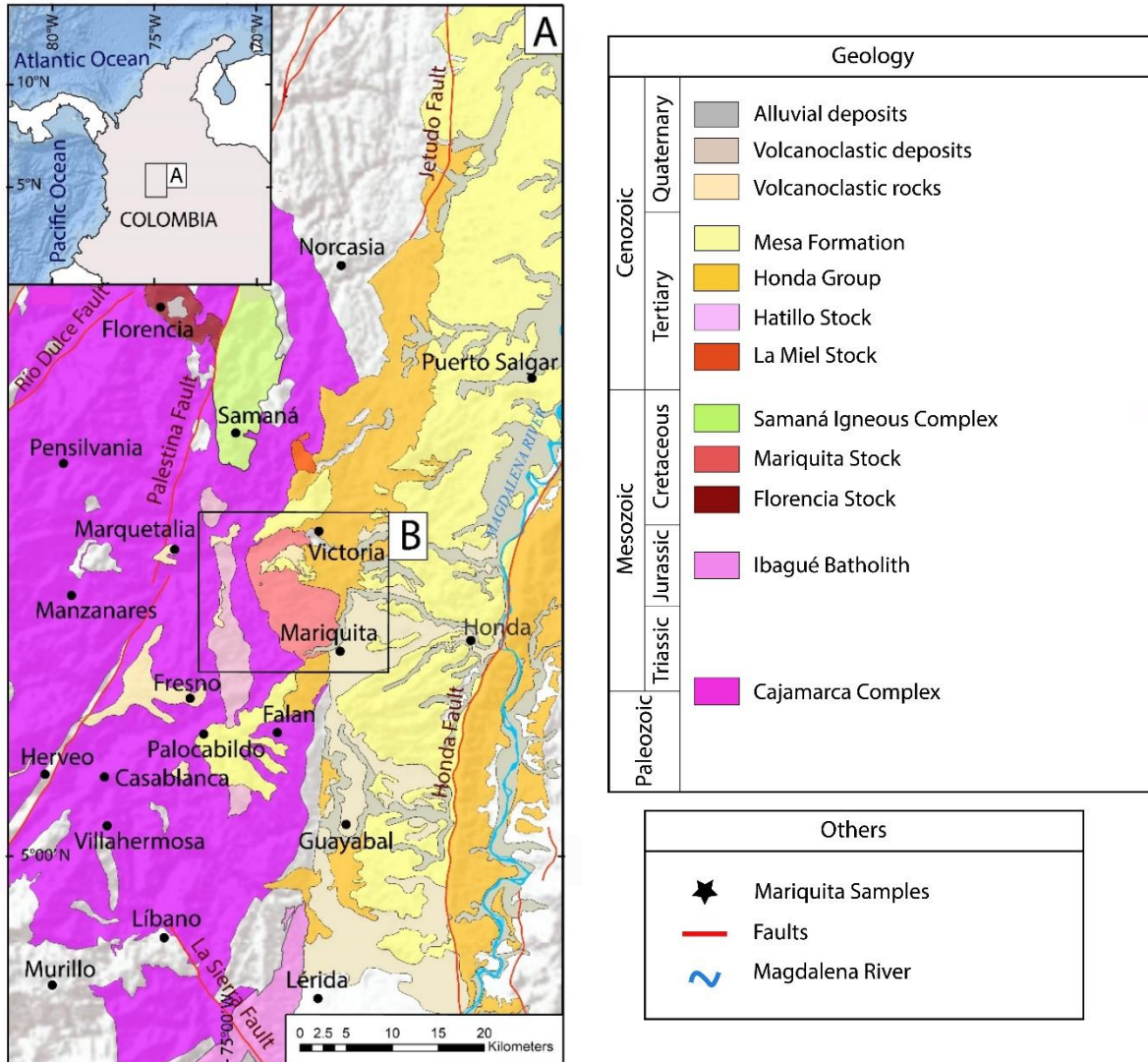


Figure 1. Regional geological map of the Mariquita stock showing the distribution of Jurassic-Early Cretaceous rocks and the studied locations.

Mariquita Stock contains tonalitic facies towards their margins, granodioritic facies towards the center of pluton and aplitic facies in contact areas (Celis et al., 2016). Barrero and Vesga (1976) described the samples of the stock as holocrystalline, leucocratic, inequigranular biotitic granodiorite, which varies locally to diorite, quartzodiorite or quartz-monzonite.

Celis et al. (2016) described the samples of Mariquita stock as granodiorite with granular-hypidiomorphic, myrmekite and perthite textures, composed of quartz (28-33%) in anhedral crystals, plagioclase (30-38%) in subhedral crystals and microcline-type feldspar (8-12%) in anhedral to subhedral crystals with alterations to kaolin. Also, post-intrusion local cataclastic event was proposed that may have affected the stock and the Cajamarca Complex inferred

by plagioclase fracture, chloritization, fractured and dislocated biotites observed in thin sections.

According to geochemical data, the samples of Mariquita stock have an acid signature, are calc-alkaline rocks due to high content of SiO₂ (68.0–73.6 wt%) and relatively high alkali contents (K₂O+Na₂O=5.37–6.96 wt%). These were classified as Granite and Granodiorite. Also, these contents low K₂O (1.8–3.0 wt%), CaO contents of (2.2–4.3wt%) values, Na₂O (3.6–4.1 wt%) and low MgO (0.7–1.8 wt%). Samples are predominantly metaluminous to slightly peraluminous supporting that the granitoids of the Mariquita Stock are I-type granitoids (Bustamante et al., 2016).

Chondrite-Normalized Rare Earth Element (REE) patterns show clear negative Eu anomalies, Light Rare Earth Elements (LREE) enrichment and flat shaped Rare-Earth Element- Heavy Rare-Earth Elements (MREE-HREE) patterns. Multi-element diagrams normalized to MORB suggest a subduction related environment and are characterized by enrichment in Large Ion Lithophile Elements (LILE) such as Rb, Th, U, K, Pb and depletion in High Field Strength Elements (HFSE) including Nb, Ti and P; likewise plagioclase-compatible elements as Ba and Sr (Bustamante et al., 2016).

Mariquita Stock intruded Cajamarca Complex Maya and González (1995) which comprises Permian-Triassic metamorphic lithologies located between the San Jerónimo fault at the west and the Otú-Pericos fault to the east. Cajamarca Complex is characterized by lithologies as slate, phyllite, quartz-muscovite schist, green schist, quartzite, gneiss, granulite, amphibolite, and marble layers. Part of the Central Cordillera basement is represented by the low to medium grade metamorphic rocks intruded by Mid to Late Triassic S-Type granitoids (Maya and González, 1995;) a (Maya and González, 1995; Vinasco., 2006; Moreno – Sánchez et al., 2008; Restrepo et al., 2011; Cochrane et al., 2014). In the study area the metamorphic rocks of Cajamarca Complex are green schists, composed by actinolite, quartz, epidote, clinozoisite, chlorite, lower proportion of opaque minerals, albite and present textures as nematoblastic and lepidoblastic and to a lesser granoblastic; grey and black schist composed by muscovite, graphite, chlorite, biotite, granoblastic texture in quartz, and other textures as lepidoblastic (Celis et al., 2016) .

Intrusive contact between the granodiorite of Mariquita and the schists of Cajamarca (Figure 1, 2) also was identified by Celis et al. (2016) due to the contact aureole which is an irregular body that comprises rocks with superimposed thermal metamorphism, . The contact aureole is composed by actinolite (55- 59% 9), quartz (8-15%), chlorite (7-10%), epidote. clinozoisite (8-15%), plagioclase (2-3%), biotite (3-5%), opaque minerals (3-11%), such as pyrite, and magnetite. The biotite content increases from 10 to 15% in some samples associated to compositional rock protolith variations, that probably corresponds to green, gray, and black schists. These rocks were classified as hornfels (Celis et al., 2016) .

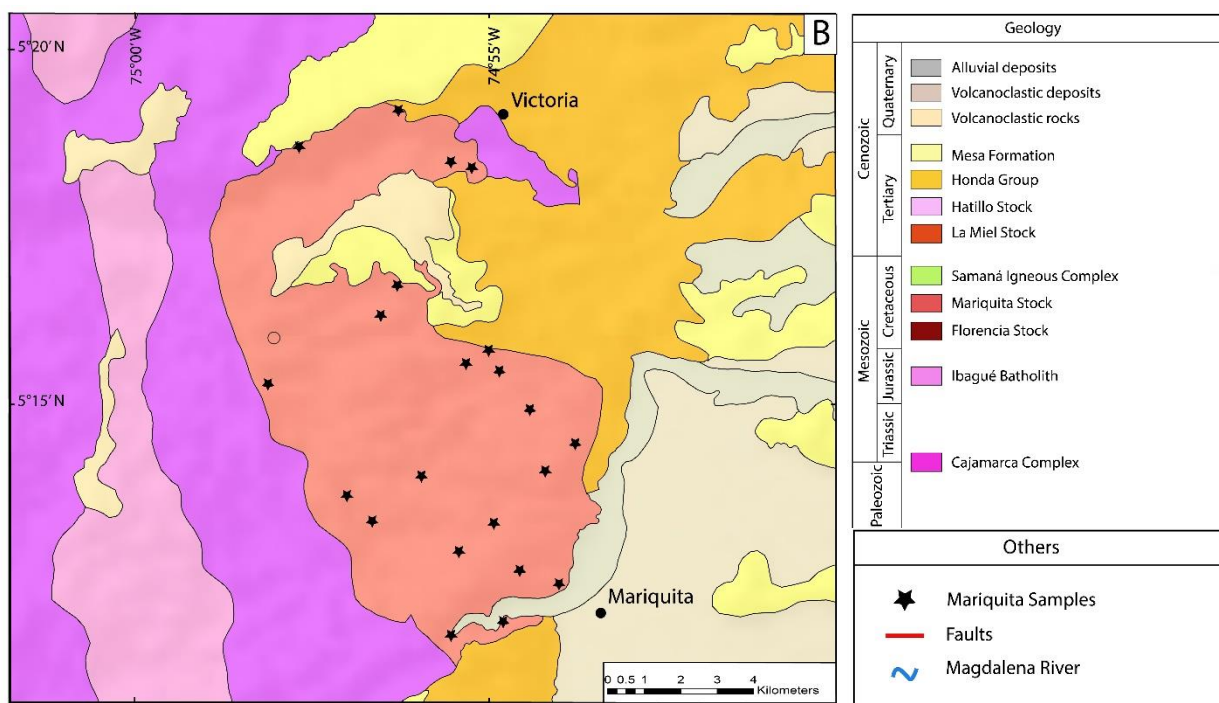


Figure 2. Local geological map of the Mariquita stock showing the units around this pluton and the samples location.

3. Analytical methods

3.1 Petrographic analyses

Petrographic analyses were obtained scanning nine thin sections and using the Image J software for petrographic description of opaque and mafic minerals, and to determine modal proportion of opaque minerals (vol%).

3.2 Whole rock geochemistry

Geochemistry data was collected from Bustamante et al., (2016) that correspond to ten representative samples of Mariquita Stock that were analyzed and plotted using the Geochemical Data ToolKit (GCDkit).

Bulk whole-rock chemical analyses of 2 samples (CM22B, CM22D) were determined, avoiding veins and weathered surfaces. The samples were crushed using a jaw crusher and powdered using a tungsten carbide ring mill. Major and trace elements were analyzed using a Rigaku 3370 X-ray fluorescence (XRF) spectrometer at Washington State University. Details of sample preparation, dilution, and analytical procedures have been described in Johnson et al. (1999). Major, trace, and rare earth element (REE) results are

reported in Table 1. REEs were determined by ICP-MS at Washington State University. A 2 g aliquot was weighed into a graphite crucible and mixed with 2 g of LiBO₂ flux. The crucibles were placed in an oven and fused at 1000 °C in a muffle furnace for 30 min. The resultant bead was ground in a steel ring mill, and a 0.25 mg portion was dissolved using HNO₃ (2 mL), HF (6 mL), and HClO₄ (2 mL) at 110 °C. Calibration standards and reagent blanks were added to the sample sequence. Sample solutions were aspirated into an ICP emission spectrograph (Jarrel Ash Atom Comb 975) for determining major oxides and certain trace elements (Ba, Nb, Ni, Sr, Sc, Y, and Zr), while the sample solutions were aspirated into an ICP-MS (Perkins-Elmer Elan 6000) for determination of the trace elements, including REEs. Therefore, both samples (CM22B and CM22D) also were analyzed and plotted using the Geochemical Data ToolKit (GCDkit).

3.3 Magnetic susceptibility

The specimens for Magnetic susceptibility (*K_m*) that were measured correspond to twelve locations in the Mariquita Stock which three cores were measured for each locality and are presented in Table 2. Eleven localities correspond to the main intrusive body and one locality correspond to a mafic enclave (CM3A, B and C). Thirty-two measurements belong to granitoid samples and three measurements belong to enclaves. The measurements were performed using a Kappabridge MFK1-FB instrument, at low field (200 A/m) and frequency operation of 976 Hz using the individual measurements mode for Bulk Susceptibility providing the mass susceptibility that controls how the measured *K_m* is normalized and enables to set the default values of the specimen mass, further was used Susceptibility Normalization option to defines how data are normalized and presented. Finally, the data were processed using Safyr 4W software version 4.0.3 and mapping *K_m*, FeO_t and SiO₂ was produced using ArcGis software using Inverse Distance Weighted (IDW) interpolation which were distributed in a quantile classification.

4. Results

4.1. Magnetic and mafic petrographic features

The main mafic mineral in the Mariquita Stock is biotite that is characterized by poikilitic texture with plagioclase crystals and hornblende crystals are in lesser proportion along the pluton. Biotite with reddish-brown pleochroism and hornblende crystals contain inclusions of opaque minerals (Figure 3.a, 3.b). Furthermore, enclaves have similar mineral assemblage than granodiorite samples but with higher contents of ferromagnesian minerals (Figure 3.c, 3.d), plagioclase and acicular apatite for CM22B enclave (Figure 3.d).

Variations in mafic crystals shapes and dimensions are notable towards the eastern and the southern margins of the pluton, where mafic grains become larger and euhedral as

seen in the CM2, CM13, CM14, CM16, CM18 samples, whereas to the center and the southwestern margin of the pluton, mafic grains are smaller and subhedral-anhedral as seen in the CM8, CM12 samples. The CM3 sample correspond to an enclave which shows several variations in shape and grains size crystals where is noticeable the porphyritic texture (Figure 4).

The total content of opaque minerals reaches up to 5% in the enclave sample (CM3) and 4% in the center and northern zones (CM12, CM20) whereas the areas with minor proportion of opaque minerals is the southern margin (CM13, CM14, CM18, CM16, CM8). In addition, the relationship between the modal proportion of opaque minerals and elevation is strongly positive ($R^2=0.1183$) and weakly positive relationship is shown with FeO_t content wt% ($R^2= 0.0485$), reflecting a vertical increase in modal opaque minerals toward the apparent roof of the pluton or the area most exposed to weathering (Figure 4).

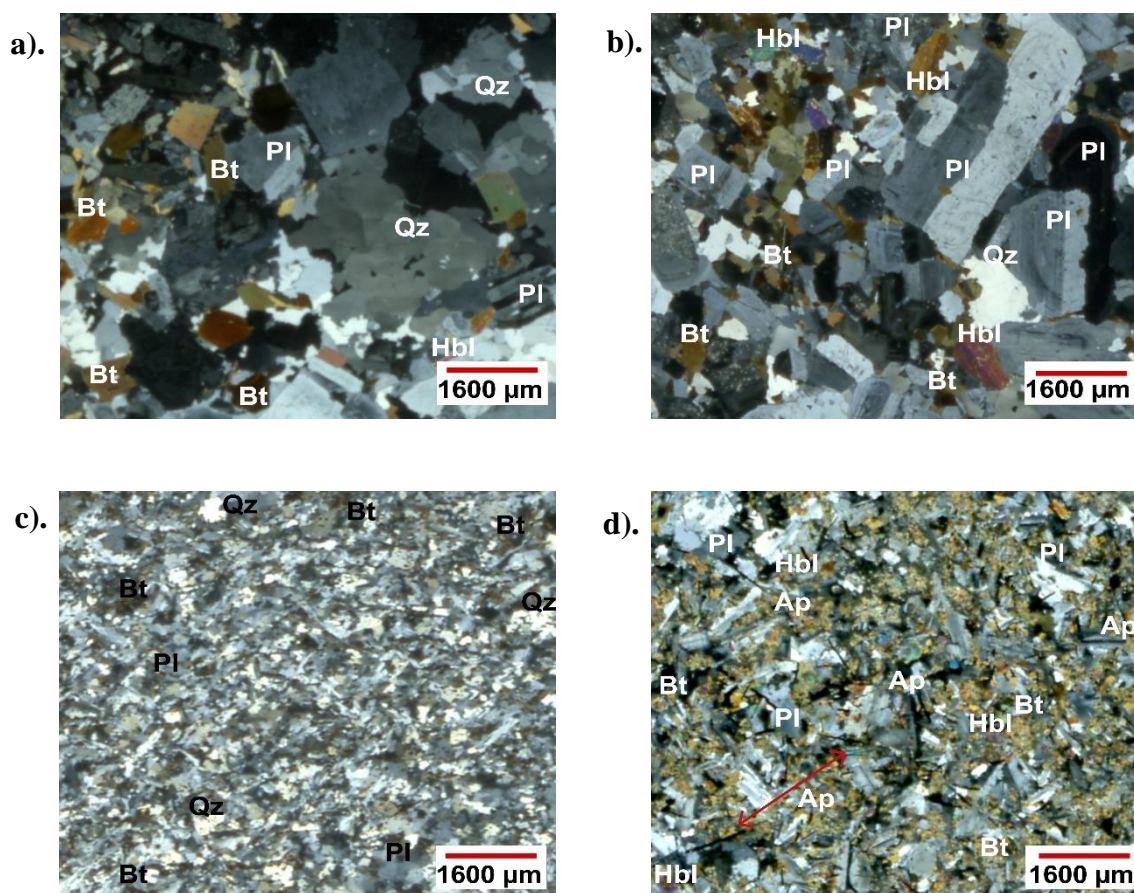


Figure 3. Thin section photographs of representative granodiorite and enclaves samples from the Mariquita stock. a). and b). Host granodiorite samples (cross-polarised light); c). Granodioritic enclave; d). Mafic enclave exhibiting acicular apatites in CM22B (cross-polarised light).

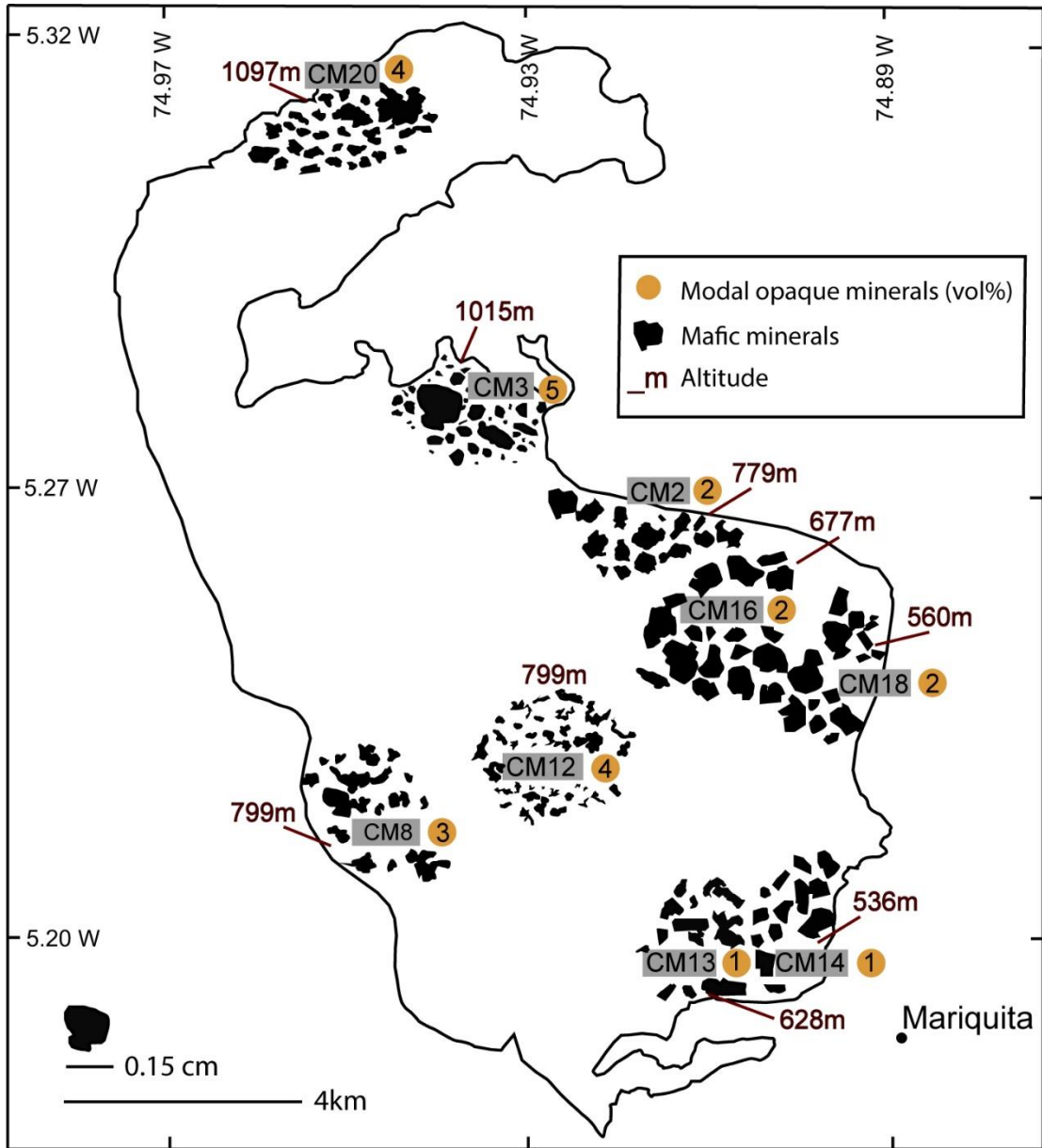


Figure 4. Distribution of modal opaque minerals (vol%) and petrographic features of mafic minerals along Mariquita stock. Red numbers means the Altitude of samples location.

Sample.:	CM22D	CM22B
SiO ₂	69.33	52.74
Al ₂ O ₃	14.54	15.01
FeO	3.66	9.67
MgO	0.98	4.94
CaO	2.47	8.07
Na ₂ O	4.18	4.36
K ₂ O	2.78	1.02
TiO ₂	0.711	2.167
P ₂ O ₅	0.244	0.295
MnO	0.067	0.187
LOI	0.50	1.06
Sum	98.96	98.45
Pb	12.11	4.23
Ba	553	189
Cs	4.60	0.87
Hf	7.16	5.17
Nb	11.24	8.21
Rb	129.4	35.0
Sr	81	254
Ta	0.86	0.63
Th	10.18	2.23
U	3.08	0.84
Zr	286	219
Y	41.37	43.55
La	29.68	12.64
Ce	62.36	31.81
Pr	8.13	4.76
Nd	31.97	22.12
Sm	7.82	6.37
Eu	0.70	2.02
Gd	7.86	7.31
Tb	1.36	1.31

Table 1. Whole-rock geochemistry from two mafic enclaves (CM22B, CM22D) of the Mariquita Stock.

4.2. Major and trace element geochemistry

According to TAS classification diagram (Middlemost, 1994), CM22B enclave plotted as Gabbroic Diorite and CM22D enclave plotted as Granodiorite (Figure 5). REE patterns normalized respect to the chondrite composition of Boyton (1984) are characterized by a slightly negative Eu anomalie for CM22B enclave while for the CM22D enclave is a strongly negative. In addition to the difference between both enclaves respect to the Eu abundance; Sr and Ti also show different behaviors between the two enclaves, for the CM22B enclave the Sr and Ti abundances are flat while for the CM22D enclave the Sr and Ti abundances are strongly negative (Figure 6.a). Multi-element patterns normalized with respect to the primitive mantle (Sun and Mc Donough, 1989) are characterized by an enrichment in LILE such as Rb, Th, U, Pb and depletion in Nb, Sr, and Ti (Figure 6.b).

Instead, geochemistry data from the Mariquita Stock was compiled from Bustamante et al. (2016), and this data suggesting that this stock is composed by Granite and Granodiorite (Figure 5) which are characterized by enrichment in Large Ion Lithophile Elements (LILE) such as Rb, Th, U, K, Pb and depletion in High Field Strength Elements (HFSE) including Nb, Ti and P; (Figure 6.a,b). In addition, the strong inverse relationship between P_2O_5 and SiO_2 suggest I-type granite signature (Figure 7.a).

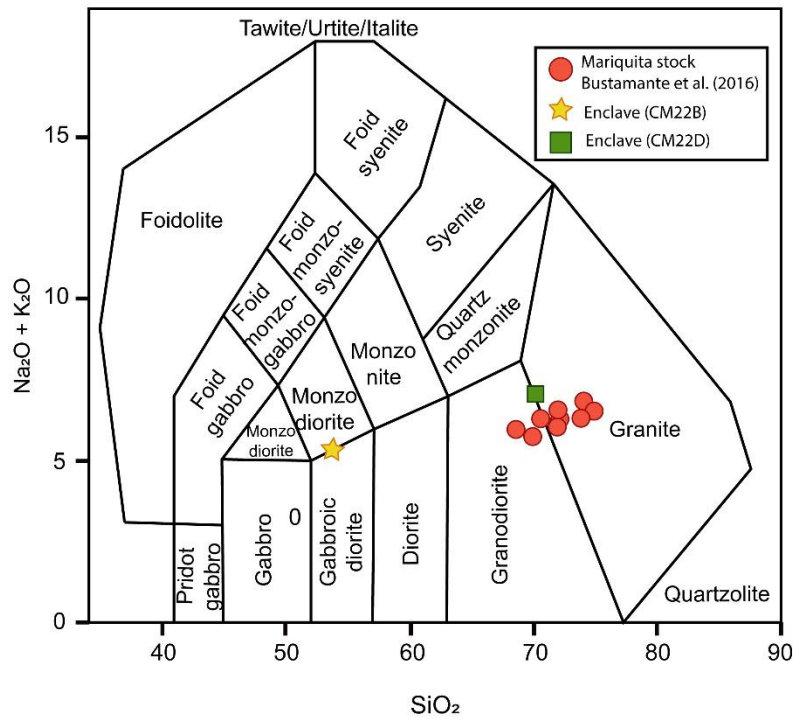
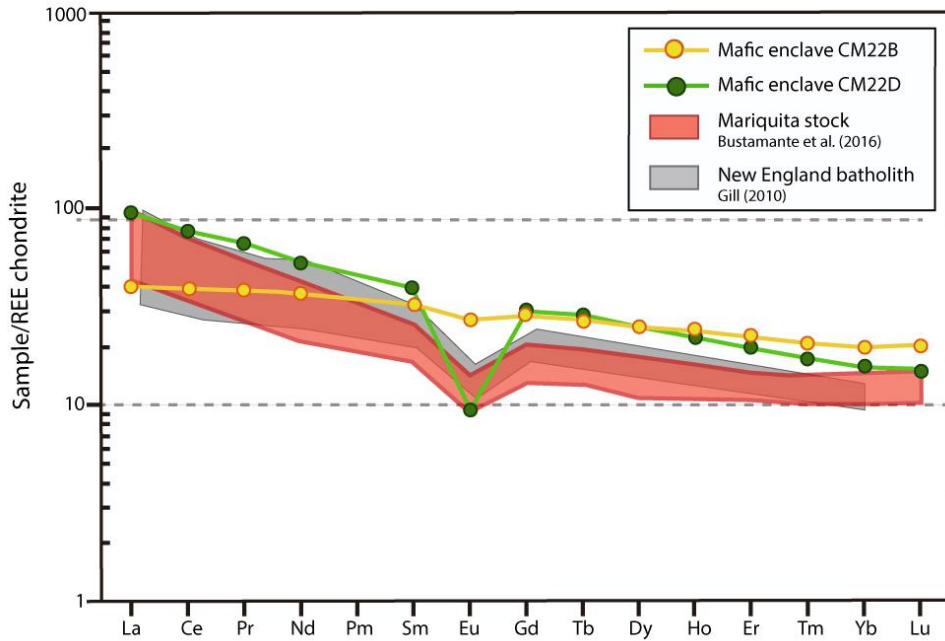


Figure 5. TAS classification diagram (Middlemost, 1994) to Mariquita stock samples.

a).



b).

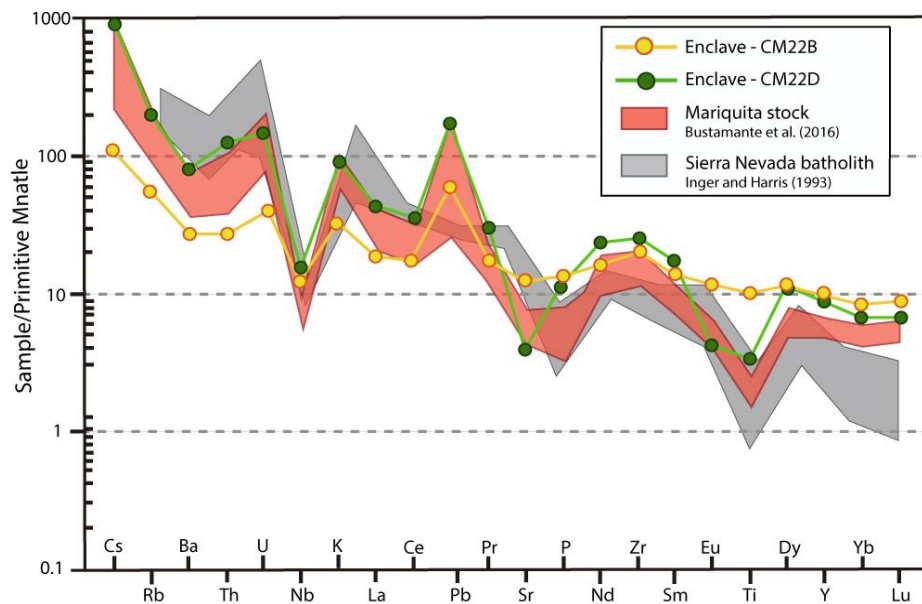


Figure 6. a). Chondrite-normalized rare earth element (Boydton, 1984). **b).** Multi-element diagrams normalized to MORB (Sun and McDonough, 1989).

Moreover, the Zr/Hf ratios from the Mariquita stock (36.11-42.70, average 38.55) are similar to the PM values proposed by McDonough and Sun (1995) which is 37, whereas the Nb/Ta from the Mariquita stock (7.5–11.14, average 8.68) are similar to the crustal values proposed by Taylor and McLennan (1985) which is 11.4.

The Rb/Sr values has an inverse relationship with Sr (Figure 7.b), indicating fractionation of plagioclase from the original magma ratifying normalized trace elements patterns

depletions in Eu, Ba and Sr. The positive correlation between Dy and Er means hornblende fractionation (Figure 7.c).

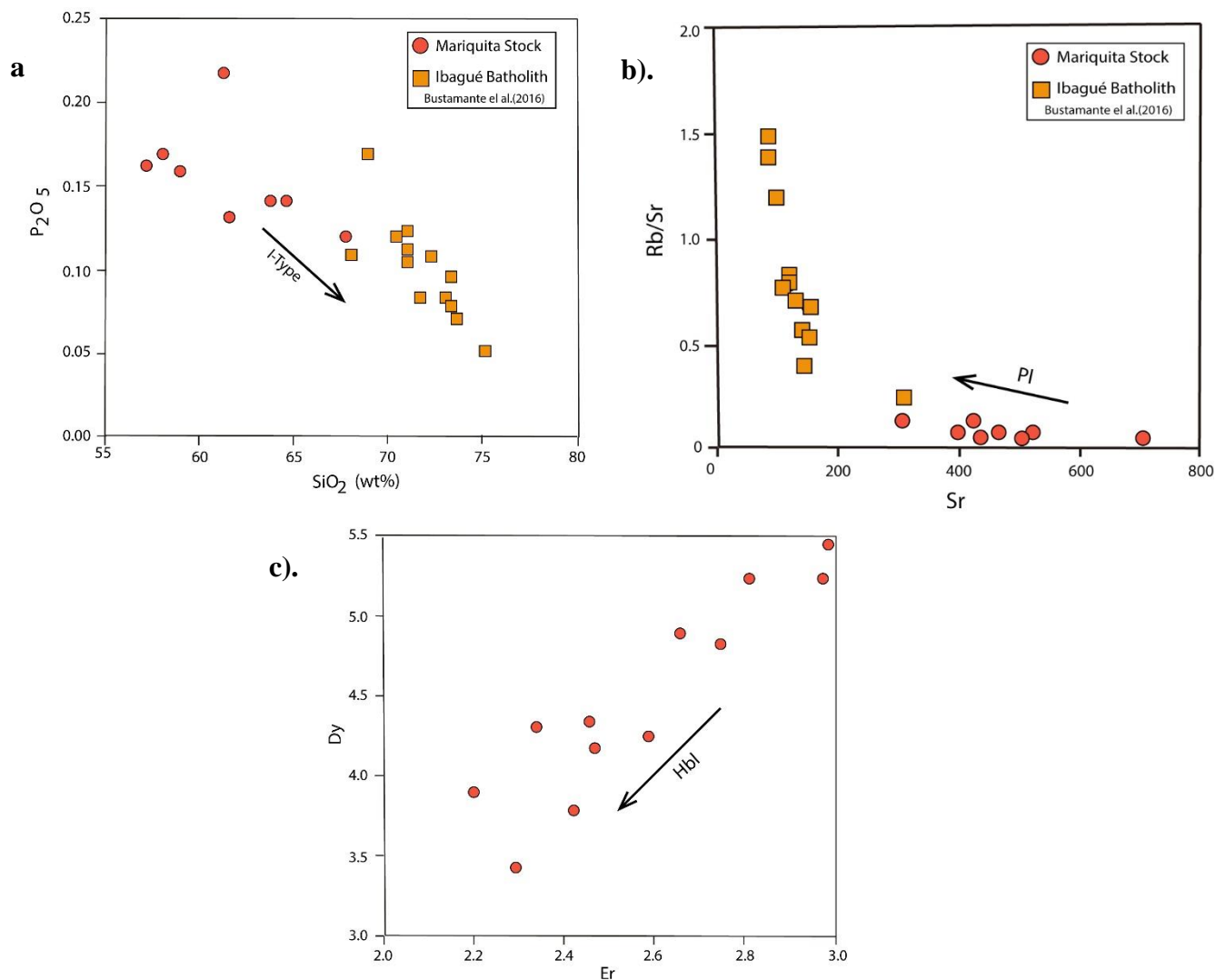


Figure 7. Binary plots of variations in the composition of granitoids. .

a). Plots of P₂O₅ respect to SiO₂ (wt%). **b).** Rb/Sr respect to Sr to Mariquita Stock and Ibagué Batholith. **c).** Plots of Dy respect to Er . Hbl arrow ,fractionation of hornblende; I-Type arrow, I-Type granitoid; Pl arrow, plagioclase fractionation.

4.3 Magnetic susceptibility

The specimens that were measured using Kappabridge MFK1-FB instrument correspond to thirty-three cores of granitoids and three cores of mafic enclaves (CM3A, B, C) in the Mariquita Stock that are presented in Table 2.

Sample .:	N	W	Km (10^{-7} [SI])
			1.72
CM2	5 16.103	-74 54.387	1.86
			1.69
			216.00
CM3	5 15.816	-74 55.128	225.00
			225.00
			1.29
CM6	5 15.459	-74 57.921	1.46
			0.99
			1.33
CM8	5 13.564	-74 57.084	1.29
			1.39
			3.43
CM12	5 13.957	-74 55.857	3.58
			3.23
			1.70
CM13	5 12.560	-74 54.526	1.32
			1.62
			1.34
CM14	5 12.484	-74 53.939	1.30
			1.42
			3.07
CM16	5 14.885	-74 54.610	2.56
			2.42
			1.42
CM18	5 14.474	-74 53.659	1.62
			1.63
			1.17
CM20	5 18.843	-74 57.264	1.11
			1.11
			14.20
CM25	5 12.002	-74 54.806	11.80
			12.90

Table 2. Magnetic Susceptibility (Km) for samples of Mariquita Stock.

The values for Mariquita Stock span from $1.11 \text{ E}^{-7} \text{ m}^3/\text{kg}$ to $0.42 \text{ E}^{-7} \text{ m}^3/\text{kg}$ (SI) (Table 2). Remarkably, the Mass Susceptibility distribution has a unimodal distribution with an interval of $1.11\text{E}^{-7} \text{ m}^3/\text{kg}$ to $3.30\text{E}^{-7} \text{ m}^3/\text{kg}$ (Figure 8). Low values dominate for 88% of the samples $Km < 1\text{E}^{-6}$ SI and only in three stations $Km > 1\text{E}^{-6}$ SI (Figure 8). Therefore, susceptibility of paramagnetic origin is dominant, due to ferromagnesian silicates (Rochette, 1987) except the three samples with high values of which one corresponds to a mafic enclave (CM3).

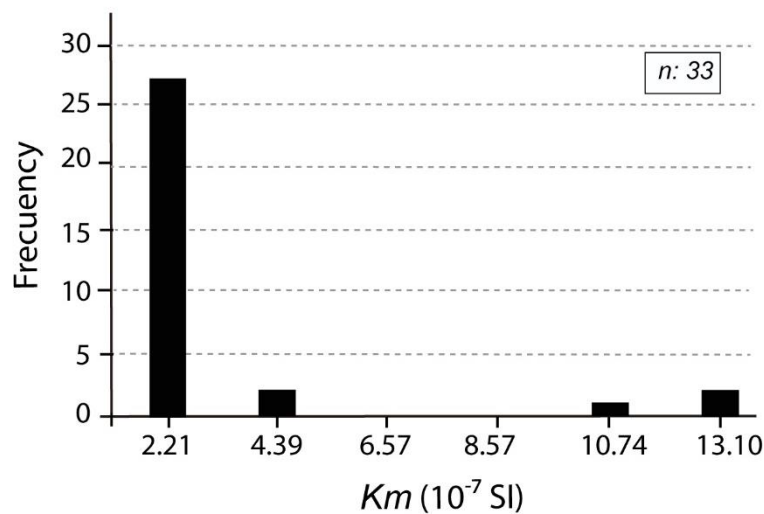


Figure 8. Frequency histogram for the magnetic susceptibility of the Mariquita Stock (Km [SI]).

Magnetic Susceptibility Map of the Mariquita Stock, without enclaves values (Figure 9.a,b,c) shown a concentric pattern where the highest values are in the center (CM12,CM16) with a marked tendency toward the eastern boundary and is correlated with unimodal distribution showed in Figure 8. In contrast, toward northwest of pluton the values are lower and appears more gradual. The magnetic measurement distribution suggest a strong similarity with the FeO_t wt% ($R^2:0.2687$) (Figure 9.a; 9.b; 10.a) and an strongly inverse relationship with the SiO_2 wt% map ($R^2:0.8914$) (Figure 9.b; 9.c; 10.b)

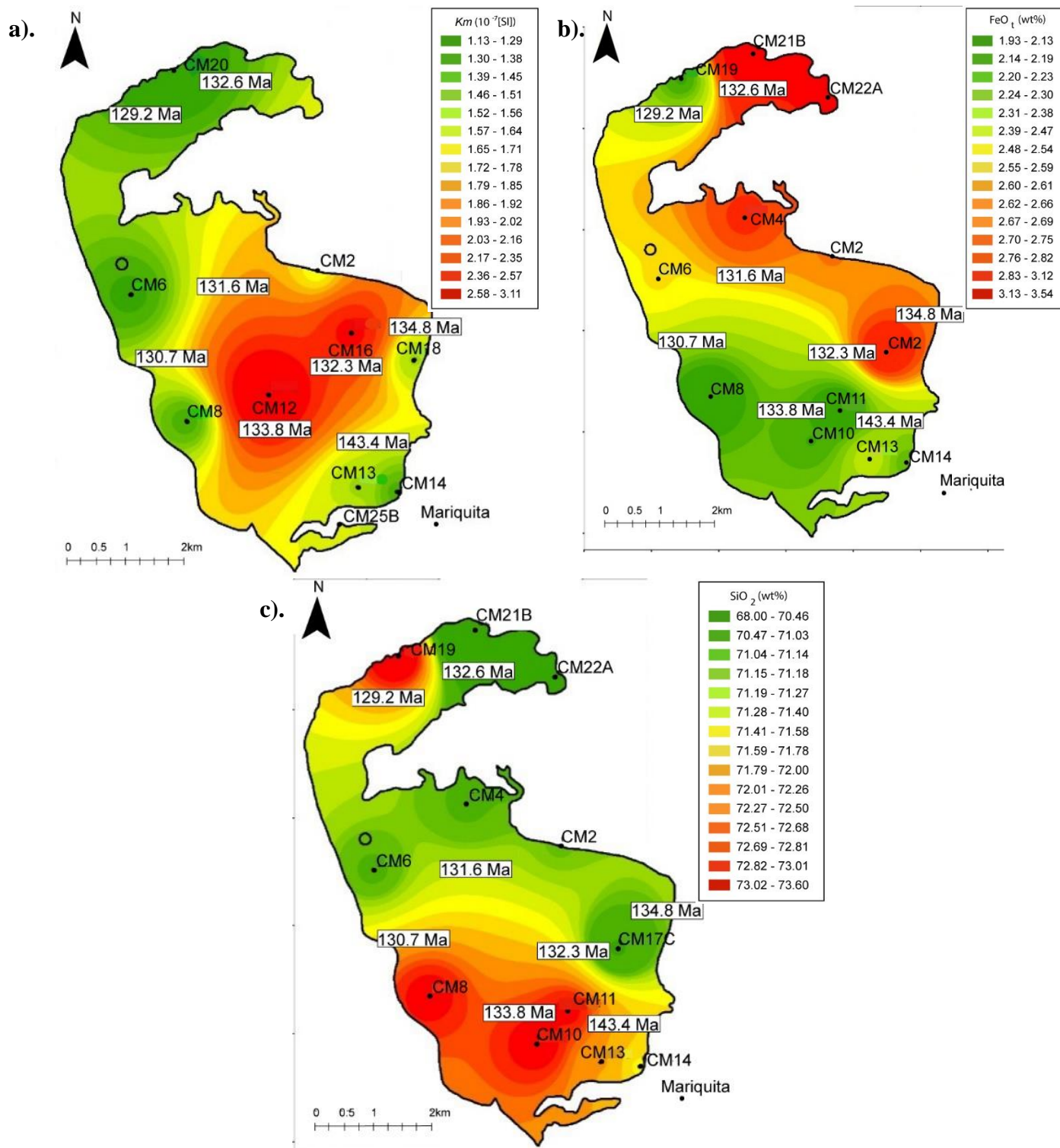


Figure 9. a) Magnetic Susceptibility map (Km [SI]). b) Map of FeO_t wt% Distribution. c) Map of SiO_2 wt% distribution across the Mariquita Stock. U/Pb crystallization ages from Bustamante et al., (2016).

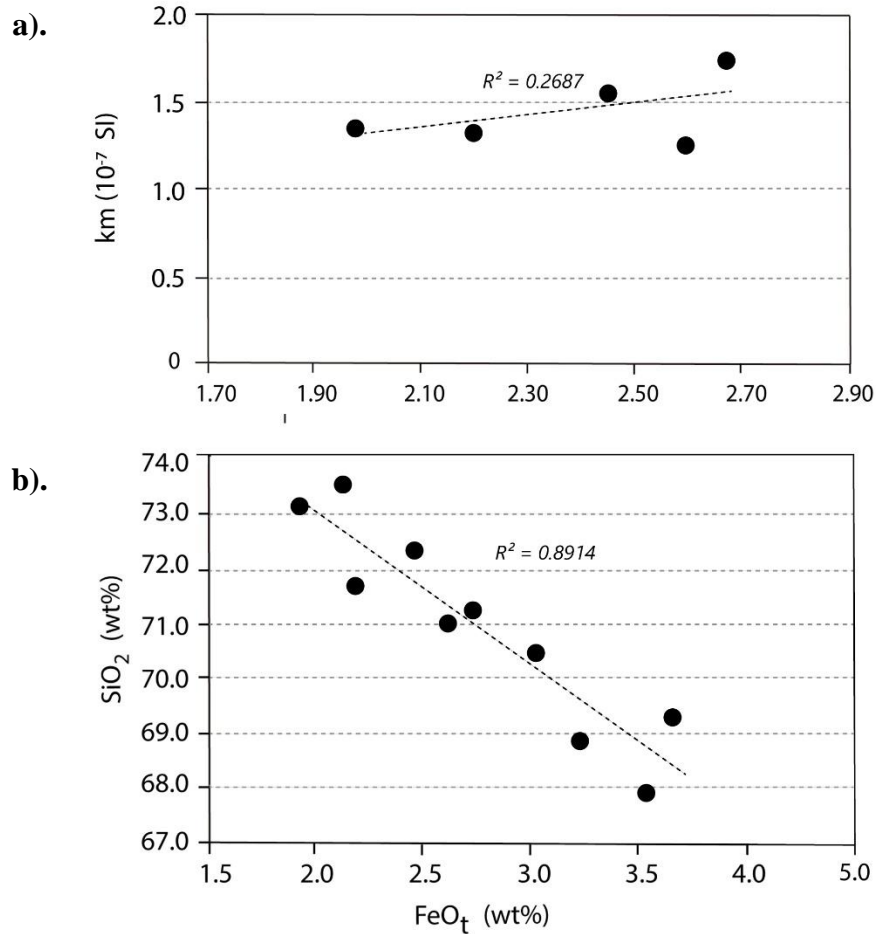


Figure 10. a) Correlation between FeOt and Km. b) Correlation between FeOt and elevation.

5. Discussion

5.1 Genesis of the Mariquita stock

Multi-element patterns normalized with respect to the primitive mantle (Sun and McDonough, 1989) are characterized by an enrichment in LILE such as Rb, Th, U, Pb and depletion in Nb, Sr, and Ti (Figure 6.a; 6.b). REE patterns normalized respect to the chondrite composition of Boyton (1984) are characterized by a slightly negative Eu anomalie for an enclave (CM22B) while for the other enclave is a strongly negative (CM22D) which may be correlated to a geochemical signature of a magmatic arc (Pearce et al., 1984).

Enclaves could be formed by mingling processes between mafic melts from a depleted region and granitic melts generated by partial melting of juvenile crustal material (He et al., 2018). In this sense, the composition of the dioritic enclave CM22D which have

strongly negative Eu, Sr and Ti anomalies (Figure 6.a; 6.b) indicate mingling processes between the deep crust and the basic end-member derived from partial melting probably of a depleted mantle source (lower crust). These trace elements features also suggest mafic mineral fractionation (Taylor and McLennan, 1985) as shows Hornblende fractionation trend in the Figure 7.c. However, CM22B have slightly flat Eu, Sr and Ti anomalies which is related with a more depleted-source (Figure 6.b).

Trace elements presented here indicate that both enclaves (CM22B and CM22D) represent different degrees of hybridization between magmas derived from pre-existing crustal material and a depleted mantle derived component. Furthermore, the depletion in Nb of two enclaves could imply interaction between the depleted mantle with melts related with subduction before partial melting (Gill, 1981).

Likewise, geochemical characteristics of the Mariquita stock reported by Bustamante et al. (2016) suggests that the geochemical signature of this pluton is related with a magmatic arc (Pearce et al., 1984) and is a I-type granitoid due to features as an enrichment in LIL-elements (Rb, Th, U, K, Pb), depletion in HFS-elements (Nb, Ti and P); and depletion in plagioclase-compatible elements such as Ba and Sr indicating fractionation of plagioclase from the magma.

This pluton has also been included within the history of the Jurassic arc magmatism of the northern Andes due to its crystallization age interval (ca. 143 to 129 Ma) that overlaps with the youngest phases of the Ibagué batholith (Bustamante et al., 2016; Rodríguez et al., 2020; Bayona et al., 2020). Below, the genesis, source characteristics and tectonic implications of this pluton will be discussed.

Contrasting features such as the high amount of silica (68.00-73.60 wt. %) and alkalis (5.37–6.96 wt.%) together with its isotopic characteristics (whole rock initial ϵ_{Hf} between +7.3 and +10.6; Bustamante et al., 2016) claims for a juvenile source with a negligible crustal contamination of the Mariquita stock and a high degree of differentiation also supported by LREE enrichment (Figure 6.a; 6.b). Highly differentiated magmatic bodies are usually related to a thick continental crust, where long residence times and slow cooling rates are favored (Farner and Lee, 2017). However, thermobarometrical calculations from Chavarria et al. (2020) from the Mariquita stock reveals that this pluton was emplaced into a thin crust. Additionally, an inverse relationship between Rb/Sr and Sr values (Figure 7.b) and depletions in Ba, Sr and Eu from Primitive Mantle-normalized trace elements patterns (Figure 6.b) imply plagioclase fractionation which is stable at shallower depths and a thin crust (Bea, 1996). This condition requires a more coherent explanation for combining the high degree of differentiation with the juvenile nature of this pluton.

Zr/Hf ratios of the Mariquita stock varies from 36.1 to 42.7 (38.4 in average) and are closer to the Primitive Mantle (PM) values (Zr/Hf=37: McDonough and Sun, 1995),

whereas Nb/Ta ratios ranges from 7.5 to 11.1 resembling those of the crust (Nb/Ta=12: McDonough and Sun, 1995). This may suggest that this pluton is derived from a mixture of depleted mantle and crustal sources, probably the lower crust and middle crust. This interpretation is supported by the similarities between the typical multielement trend and the crust (Figure 11) (Taylor and McLennan, 1995; Wedepohl, 1995; Rudnick and Gao, 2003; White, 2014) its negative Nb, Ti anomalies and positive Pb anomaly although this could be also related to the influence of the fluids in the subduction zone on the primary source (Figure 6.a; 6.b). Furthermore, Hf and Nd isotopic data reported by Bustamante et al. (2016) are in accordance with such a depleted source. These authors interpreted such a juvenile character of the Mariquita stock with a reduction of the fusible elements (i.e. sediments) in the source related to a more oblique convergence between the Farallón plate and NW South America by the end of the Jurassic. We add another clue that may help to explain the high degree of differentiation while the juvenile source remained unaffected and is the fact that this pluton is intruding greenschists of Cajamarca Complex (Figure 2) (Bustamante et al., 2016; Celis et al., 2016) preventing any substantial assimilation during the differentiation process to change its juvenile isotopic signature.

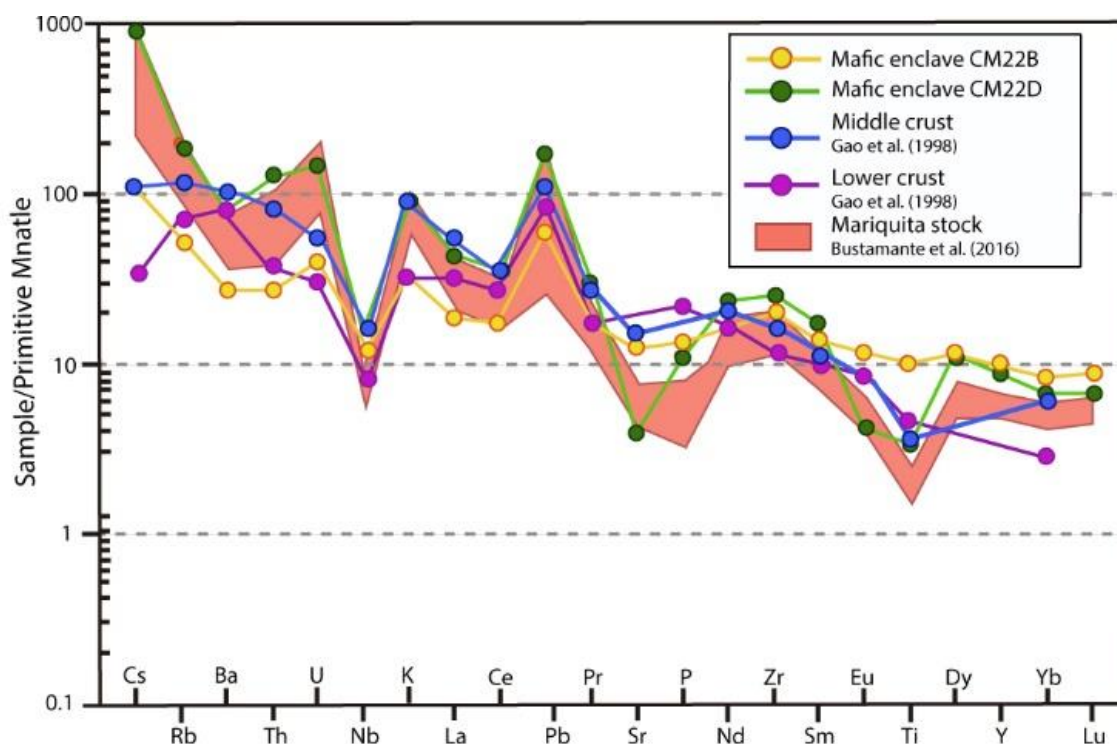


Figure 11. Multi-element diagrams normalized to MORB (Sun and McDonough, 1989). Correlation of Mariquita stock samples with Middle crust and Lower crust trends.

the development of chilled margins against the host granites, their elongate shape, the absence of solid-state deformation and the presence of microscopic acicular in the pluton and two enclaves implying that mafic melts were injected into and mingled with the granodioritic magma a (Lowell, 1999).

Nonetheless, the fact that Mariquita stock was emplaced into a thin crust (Chavarria et al., 2020) and has a juvenile isotopic signature (+5ENd; Bustamante et al. 2016) implies that this pluton was close to the trench due to isotopically juvenile, similar to the Andes trend which is most isotopically juvenile closest to the trench (Stern, 1991; Kay et al., 2005; Boekhout et al., 2015; Jones et al., 2015) and most of the petrogenetic models for cordilleran systems where the spatial isotopic trend is intrinsic attribute of architecture and tectonic history of mantle lithospheric (Chapman et al., 2017).

5.2 The magnetic properties of the Mariquita stock and their implications

The subtle internal architecture of plutons can be detected from magnetic susceptibility (Km) analyses taking into consideration that variations in the oxidation state of parental granite magmas is primarily controlled by the source region and on the geodynamic scenario, where features across plutonic bodies such as multiple magmatic pulses, magma mixing, assimilation, magmatic differentiation or contrasting oxygen fugacity can play a significant role (Ishihara, 1981; 2001; Gleizes et al., 1993; Pichavant et al., 1996; Aydin et al. 2007; Ferre et al., 2012; Kelley and Cottrell, 2012; Ernst, 2013; Villaseca et al., 2017).

In that sense, an approximation to mapping of a granite pluton is possible considering the frequency of Km , their correlation with height above sea level and petrographic characterization analysis that is related with the cumulative distribution of magnetic minerals, hence abundance, nature, and chemical composition (Figure 12) (Dél ris et al., 1996; Villaseca et al., 2017) which have been explained by differences in the oxygen fugacity of magmas (Ishihara, 1981; Jin, 2001). Likewise, a weakly positive correlation of modal opaque minerals with elevation in the Mariquita stock reflects a vertical increase in modal opaque minerals toward the apparent roof of the pluton or the area most exposed to weathering and an upward variation in magma composition that is supported by the positive correlation between bulk-rock FeO_t and magnetic susceptibility (Figure 10; 12) ($R^2 = 0.268$). This increase in the magnetic susceptibility from the lower to higher values about $1.25E^{-7}$ to $1.75 E^{-7}$ that is consistent to whole rock FeO_t increase of 3,71% between the same samples. Values reported for magnetic susceptibility in granites around the world range widely from 10^{-6} SI in leucocratic granites up to 10^{-1} (Tarling and Hrouda, 1993; Gleizes et al., 1993; Borradaile and Henry, 1997; Bouchez, 1997; Gregorova et al., 2003). The Mariquita stock samples reported in this work ranges from $1.11 E^{-7}$ [SI] to $3.30 E^{-7}$ [SI]. According to Gleizes et al. (1993) peaks of frequency distribution could indicate

different magmatic pulses and in this case, the samples studied show an unimodal distribution ($2.21E^{-7}$ SI) that suggests a main magmatism pulse, whereas a minor pulse could be represented by the enclaves (Km values of $4.39 E^{-7}$, $1.07 E^{-6}$ and $1.31 E^{-6}$ SI) (Figure 8; 9).

An additional feature is that the iron content is the main geochemical control of the magnetic susceptibility in magmas, and mafic and opaque minerals are the main bearer of magnetic susceptibility. As FeO_t decreases during magmatic differentiation, the magnetic susceptibility decreases as well (Aydin et al., 2007). This is evidenced in the Mariquita stock where magnetic distribution suggests a strong similarity with FeO_t wt% and an inverse relationship with SiO_2 wt% ($R^2= 0.89$)(Figure 9; 10).

The mafic minerals exhibit euhedral to subhedral shapes, and those variations in mafic grains shapes are notable towards the southern and the eastern margin of the pluton, where mafic grains become larger and euhedral, whereas towards the southwestern margin, mafic grains are smaller and subhedral (Figure 3;4). Probably, these variations correspond to contrasts in fO_2 which affect Fe oxides stability in plutonic rocks (Frost, 1987; Williams et al., 1989) due to the fO_2 is internally controlled by multivariant equilibria involving the silicates, the oxides and the melt (Frost, 1991), as show the FeO map and the distribution of the magnetic susceptibility indicating that the most differentiated zones are located towards northwest and southwest of the pluton (Figure 9).

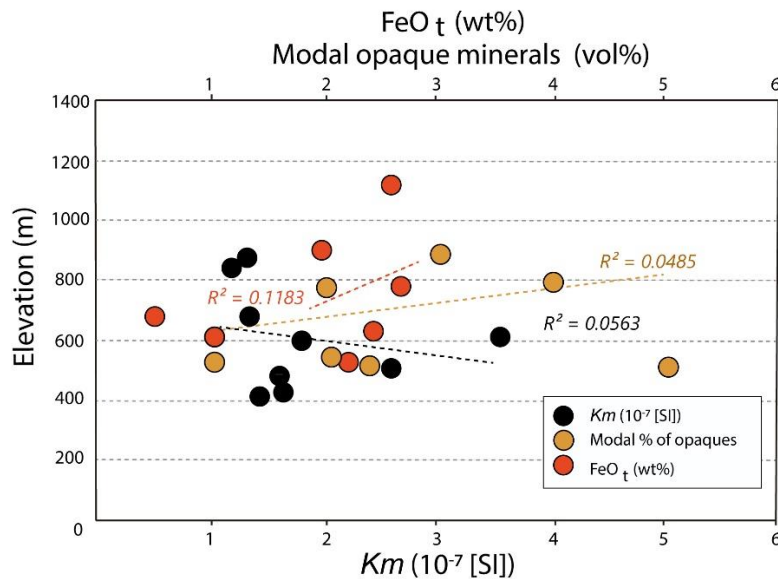


Figure 12. Correlation between modal proportions iron oxides and FeO_t respect to high above sea level.

Different authors have proposed that granitoids could be classified into magnetite or ilmenite series and it is used to refer to two types of granitoids whose magmas evolved under distinct oxygen fugacities (Read, 1949; Buddington 1959; Ishihara, 1981). Mariquita

samples correspond to the ilmenite field according to the Km values showed in Table 2 and values classification by Ishihara (1981); Gregorová et al. (2003).

In the ilmenite series, the Km values are lower than $3E^{-3}$ [SI], the plutonic bodies are highly differentiated, and are related with emplacement at shallow depths, near the trench and are characterized by reddish biotite pleochroism as in the Mariquita stock. In contrast, magnetite series, the Km values are higher than $3E^{-3}$ [SI], the plutonic bodies are undifferentiated, and are related with emplacement at higher depths, away from the trench and are characterized by greenish biotite pleochroism (Ishihara and Ulriksen, 1980; Ishihara, 1981; Ishihara et al., 2002; Takagi, 2004; Ishihara, 2007).

6. Conclusions

New magnetic susceptibility data combined with geochemical analysis and modal opaque minerals disclose that (Figure 13) (1) Mariquita stock was emplaced near the trench during an Jurassic- Early Cretaceous shutdown and it was subjected to mingling processes between the deep crust and the basic end-member derived from partial melting probably of a depleted mantle source (lower crust). (2) The permanence of the juvenile character while the prolonged magmatic differentiation is due to the intrusion of the pluton into greenschist rocks.

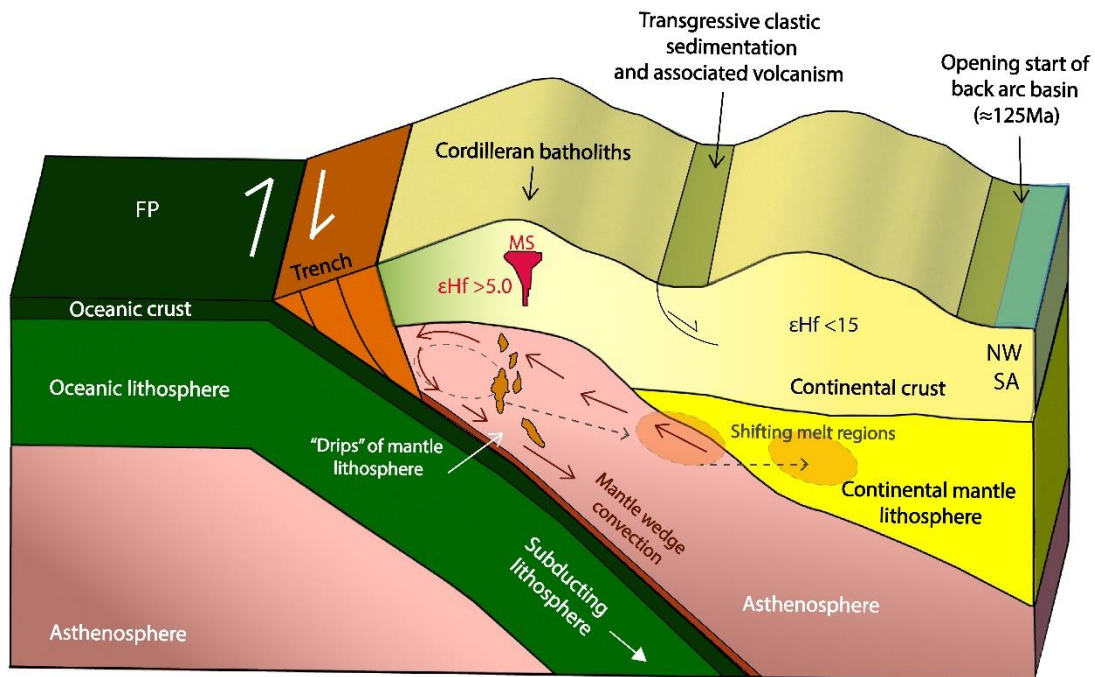


Figure 13. Tectonic scenario proposed to the Mariquita stock. Modified from Chapman et al. (2017); Jaramillo et al. (2017); Cardona et al. (2020). (MS) Mariquita stock. (FP) Farallon Plate. (NW SA) Northwestern margin of South America.

- (3) Correlation between modal opaque minerals and magnetic susceptibility indicates that studied pluton classifies as ilmenite series, even having some features of magnetite series.
- (4) Areal distribution of magnetic susceptibility data reveals that samples from the Mariquita stock at greater heights are richer in magnetic elements, opaque minerals and FeO_t content due to Km , $\text{FeO}_t/\text{SiO}_2$ maps show magmatic differentiation zones.

References

- Aspden, J.A., McCourt, W.J., Brook, M., 1987, Geometrical control of subduction related magmatism: The Mesozoic–Cenozoic plutonic history of western Colombia: *Journal of the Geological Society of London*, v. 144, p. 893–905, doi: 10.1144/gsjgs.144.6.0893.
- Aydin, A., Ferré E.C., Aslan, Z., 2007, The magnetic susceptibility of granitic rocks as a proxy for geochemical composition: example from the Sahuran granitoids, NE Turkey. *Tectonophysics*, v. 441, p. 85–95.
- Barrero, D., Vesga, C.J., 1976, Mapa geológico del cuadrángulo K-9, Armero y mitad sur del J-9, La Dorada. Escala 1:100.000. INGEOMINAS. Bogotá.
- Bayona, G., Bustamante, C., Nova, G., Salazar–Franco, A.M., 2020, Jurassic evolution of the northwestern corner of Gondwana: Present knowledge–future challenges in studying Colombian Jurassic rocks. In: Gómez, J., Pinilla–Pachon, A.O. (editors), *The Geology of Colombia*, v. 2 Mesozoic. Servicio Geológico Colombiano, Publicaciones Geológicas Especiales, p. 36, 37. Bogotá. <https://doi.org/10.32685/pub.esp.36.2019.05>.
- Bea, F., 1996, Residence of REE, Y, Th and U in Granites and Crustal Protoliths; Implications for the Chemistry of Crustal Melts. *Journal of Petrology*, v. 37, doi: 10.1093/petrology/37.3.521.
- Borradaile, G. J., Henry, B., 1997, Tectonic applications of magnetic susceptibility–its anisotropy. *Earth-Science Reviews*, v. 42(1-2), p. 49-93.
- Bouchez, J. L., 1997, Granite is never isotropic: an introduction to AMS studies of granitic rocks. In *Granite: from segregation of melt to emplacement fabrics*, Springer, Dordrecht, p. 95-112.
- Boynton, W. V., 1984, Cosmochemistry of the rare earth elements: meteorite studies. In *Developments in geochemistry*, Elsevier, v. 2, p. 63-114.
- Buddington, A. F., 1959, Granite emplacement with special reference to North America. *Geological Society of America Bulletin*, v. 70 (6), p. 671-747.

Bustamante, C., Archanjo, C.J., Cardona, A., Vervoort, J.D., 2016, Late Jurassic to Early Cretaceous plutonism in the Colombian es: A record of long-term arc maturity. *GSA Bulletin*, v. 128, no. 11/12, doi: 10.1130/B31307.1.

Cardona-Molina, A., Cordani, U.G., Macdonald, W., 2006, Tectonic correlations of pre-Mesozoic crust from the northern termination of the Colombian es, Caribbean region. *J. South Am. Earth Sci.*, v. 21, p. 337-354.

Cardona, A., León, S., Jaramillo, J.S., Valencia, V., Zapata, S., Pardo-Trujillo, A., Schmitt, A.K., Mejía, D., Arenas, J.C., 2020, Cretaceous record from a Mariana- to an Andean-type margin in the Central Cordillera of the Colombian Andes. In: Gómez, J. & Pinilla-Pachon, A.O. (editors), *The Geology of Colombia, Mesozoic*. Servicio Geológico Colombiano, Publicaciones Geológicas Especiales, v. 2, doi: <https://doi.org/10.32685/pub.esp.36.2019.10>.

Celis, S.A., Giraldo, C.A., Toro, L.M., Osorio, E., 2016, Petrografía y cartografía de la aureola de contacto de la Granodiorita de Mariquita (departamento del Tolima, Cordillera Central colombiana). *Bol. Geología, Cordilleras of Colombia*. Science Direct, v. 38(3), p. 31-40 doi:10.1016/j.lithos.2011.05.003.

Chapman, J.B., Ducea, M.N., Kapp, P., Gehrels, G.E. DeCelles, P.G., 2017, Spatial temporal radiogenic isotopic trends of magmatism in Cordilleran orogens. *Gondwana Research*, v. 48, p. 189–204. <https://doi.org/10.1016/j.gr.2017.04.019>.

Chavarría, L. F., 2020, Jurassic to early Cretaceous crustal thickness in the Colombian Northern Andes: insight on the magmatic thermal variations emplacement conditions of plutonic rocks (Doctoral dissertation, Universidad Eafit).

Cochrane, R., Spikings, R., Gerdes, A., Ulianov, A., Mora, A., Villagómez, D., Putlitz, B., Chiaradia, M., 2014, Permo- Triassic anatexis: continental rifting the disassembly of western Pangea, *Lithos*, v.190/191, p. 383-402.

Cordani, U., Cardona, A., Jiménez, D.M., Liu, D., Nutman, A., 2005, Geochronology of Proterozoic basement inliers in the Colombian es: tectonic history of remnants of a fragmented Grenville belt. *Geol. Soc. Lond. Spec. Publ.*, v. 246, p. 329-346.

Cretaceous: Influence of previous tectonic processes:

Délérís, J., Nédélec, A., Ferré, E., Gleizes, G., Ménot, R. P., Obasi, C. K., Bouchez, J. L., 1996, The Pan-African Toro Complex (northern Nigeria): magmatic interactions structures in a bimodal intrusion. *Geological Magazine*, v. 133(5), p. 535-552.

Ducea, M. N., 2001, The California arc: Thick granitic batholiths, eclogitic residues, lithospheric-scale thrusting, magmatic flare-ups. *GSA today*, v. 11(11), p. 4-10.

Ducea, M.N., Saleeby, J.B., Bergantz, G., 2015, The Architecture, Chemistry, Evolution of Continental Magmatic Arcs. *Annu. Rev. Earth Planet.*, v. 43, p. 10.1–10.33.

Ernst, W. G., 2013, Petrogenesis of the Barcroft pluton, northern White-Inyo Mountains, east-central California. *Contributions to Mineralogy Petrology*, v. 165(3), p. 419-435.

Farner, M. J., Lee, C. T. A., 2017, Effects of crustal thickness on magmatic differentiation in subduction zone volcanism: a global study. *Earth Planetary Science Letters*, 470, 96-107.

Ferré, E. C., Michelsen, K. J., Ernst, W. G., Boyd, J. D., Canon-Tapia, E., 2012, Vertical zonation of the Barcroft granodiorite, White Mountains, California: Implications for magmatic processes. *American Mineralogist*, 97(7), 1049-1059.

Frost T. P., Mahood G. A., 1987, Field, chemical, physical constraints on mafic-felsic magma interaction in the Lamarck Granodiorite, Sierra Nevada, California. *Geol Soc Am Bull* 99: 272–291.

Frost, B.R., 1991, Chapter 1. INTRODUCTION TO OXYGEN FUGACITY AND ITS PETROLOGIC IMPORTANCE. In *Oxide Minerals*. Berlin, Boston: De Gruyter. doi: <https://doi.org/10.1515/9781501508684-004>.

Gao, S., Zhang, B.R., Jin, Z.M., Kern, H., Luo, T.C., Zhao, Z.D., 1998, How mafic is the lower continental crust? *Earth and Planetary Science Letters*, v. 106, p. 101-117.

Gill, J.B., 1981, *Minerals and Rocks*. Berlin, Heidelberg, New York: Springer-Verlag. *Geological Magazine*, v. 119(5), p. 516-517, doi:10.1017/S0016756800026911

Gleizes, G., Nédélec, A., Bouchez, J. L., Autran, A., Rochette, P., 1993, Magnetic susceptibility of the Mont-Louis orra ilmenite-type granite (Pyrenees): A new tool for the petrographic characterization regional mapping of zoned granite plutons. *Journal of Geophysical Research: Solid Earth*, 98(B3), 4317-4331.

Gorczyk, W., Willner, A.P., Gerya, T.V., Connolly, J.A.D., Burg, J.P., 2007, Physical controls of magmatic productivity at Pacific-type convergent margins: Numerical modelling. *Physics of the Earth Planetary Interiors*, v. 163, p.209–232. doi:10.1016/j.pepi.2007.05.010.

Gregorová, D., Hrouda, F., Kohút, M., 2003, Magnetic susceptibility geochemistry of Variscan West Carpathian granites: implications for tectonic setting. *Physics Chemistry of the Earth, Parts A/B/C*, 28(16-19), 729-734.

He, Y., He, Z.H., Ge, W.C., Yang, H., Wang, Z.H., Dong, Y., Bi, J.H., Zhao, D., 2018, Petrogenesis tectonic implication of Late Jurassic-Early Cretaceous granitic magmatism in the Xing'an Block, NE China: Geochronological, geochemical Hf isotopic evidence. *Can. J. Earth Sci.*, 571–588.

Hiesh, P.S., Chen, C.H., Yang, H.J., Lee, C.Y., 2008, Petrogenesis of the Nanling Mountains granites from South China: Constraints from systematic apatite geochemistry whole-rock geochemical Sr-Nd isotope compositions. *Journal of Asian Earth Sciences*. doi:10.1016/j.jseaes.2008.02.002, 428–451.

Hildreth, W., Moorbath, S. Crustal contributions to arc magmatism in the es of Central Chile. *Contr. Mineral. Petrol.* 98, 455–489 (1988). <https://doi.org/10.1007/BF00372365>.

Ishihara, S., Ulriksen, C.E., 1980, The magnetite series and ilmenite series granitoids in Chile. *Min. Geol.*, v. 30, p. 183--190.

Ishihara, S., 1981, The granitoid series mineralization. *Economic Geology*. v. 1981, pp.458-484.

Ishihara, S., JIN, M. S., LEE, Y. S., 2001, Granitoids their magnetic susceptibility in South Korea. *Resource Geology*, 51(3), 189-203.

Ishihara, S., Laurence, J.B., Anhaeusser, C.R., Imai, A., 2002, Granitoid series evaluation of the Archean Johannesburg Dome granitoids, South Africa. *Bull. Geol. Surv. Japan*, v. 53(1), p. 1-9.

Ishihara, S., 2007, Origin of the Cenozoic–Mesozoic magnetite-series and ilmenite-series granitoids in East Asia. *Gondwana Research*, v. 11, p. 247-260, doi: 10.1016/j.gr.2006.04.003.

Jaillard, E., Soler, P., Carlier, G., Mourier, T., 1990. Geodynamic evolution of the northern central Andes during early to middle Mesozoic times: a Tethyan model. *Journal of the Geological Society*, v.147, doi: 10.1144/gsjgs, 1009-1022.
Journal of South American Earth Sciences, v. 29, no. 2.

Jaramillo, J.S., Cardona, A., León, S., Valencia, V., Vinasco, C. 2017, Geochemistry and geochronology from Cretaceous magmatic and sedimentary rocks at 6° 35' N, western flank of the Central Cordillera (Colombian Andes): Magmatic record of arc growth and collision. *Journal of South American Earth Sciences*, v. 76, p. 460–481, <https://doi.org/10.1016/j.jsames.2017.04.012>.

Kelley, K. A., Cottrell, E., 2012. The influence of magmatic differentiation on the oxidation state of Fe in a basaltic arc magma. *Earth Planetary Science Letters*, v. 329, p. 109-121.

Kerr, A.C., Marriner, G.F., Trney, J., Nivia, A., Saunders, A.D., Thirlwall, M.F., Sinton, C.W., 1997. Cretaceous basaltic terranes in Western Cordillera: elemental, chronological Sr-Nd isotopic constraints on petrogenesis. *J. Petrology*, v. 38, p. 677-702.

Leal-Mejía, H., 2011, Phanerozoic Gold Metallogeny in the Colombian es: A Tectono-Magmatic Approach [Ph.D. thesis]: Barcelona, Spain, Universitat de Barcelona, p. 1000.

Leal-Mejía, H., Shaw, R. P., Draper, J. C. M., 2019, Spatial-temporal migration of granitoid magmatism the Phanerozoic tectono-magmatic evolution of the Colombian es. In *Geology Tectonics of Northwestern South America*, p. 253-410.

Li, X.H., Chung, S.L., Zhou, H., Lo, C.H., Liu, Y., Chen, C.H., 2014, Jurassic intraplate magmatism in the southern Hunan-eastern Guangxi: $^{40}\text{Ar}/^{39}\text{Ar}$ dating, geochemistry, Sr-Nd isotopes implications for the tectonic evolution of SE China. *Geological Society of London, Special Publications*, v. 226, p. 193-215, doi: 10.1144/GSL.SP.2004.226.01.11.

Lowell, G., 1999, Interaction between coeval mafic and felsic melts in the St. Francois Terrane of Missouri, USA. *Precambrian Research*, v. 95, p. 69-88.

Mamami, M., Wörner, G., Sempere, T., 2009, Geochemical variations in igneous rocks of the Central ean orocline (13°S to 18°S): Tracing crustal thickening magma generation through time space. *Geological Society of America*. v. 122, p. 162–182doi: 10.1130/B26538.1.

Martens, U., Restrepo, J., Ordóñez, O., Correa, A.M., 2014, The Tahamí Anacona terranes of the Colombian es: missing links between the South American Mexican Gondwana margins. *J. Geol.*, v. 122, p. 507-530.

Maya, M., Gozález, H., 1995, Unidades litodémicas en la Cordillera Central de Colombia. *Bol. Geol.*, v. 35, p. 43-57.

McCourt, W. J., Aspden, J. A., 1983, A plate tectonic model for the Phanerozoic evolution of central southern Colombia. 10th Caribbean Geological Conference, Cartagena, Abstracts.

McCourt, W. J., 1984, A Palaeozoic paired metamorphic belt in the Central Cordillera of Colombia. *British Geological Survey Report Series*, v. 16/1, p. 22-7.

McDonough, W. F., Sun, S. S., 1995, The composition of the Earth. *Chemical geology*, v. 120, no. 3-4, p. 223-253.

Mejía, H. L., 2011, Phanerozoic gold metallogeny in the colombian es: a tectono-magmatic approach (Doctoral dissertation, Universitat de Barcelona).

Moreno-Murillo, J.M., 2010, Magmatic evolution of

Núñez, A., Bocanegra, A., Gómez, J., 1996, Los Plutones Jurásicos del Valle Superior del Magdalena (Colombia). *Final Proc. Int. Conf. Colombia*, p. 226-239.

Ordóñez-Carmona, O., Restrepo, J.J., Pimentel, M.M., 2006, Geochronological isotopical review of pre-Devonian crustal basement of the Colombian es. *J. South Am. Earth Sci.* v. 21, p. 372-382, doi:10.1016/j.jsames.2009.02.003.

Pichavant, M., Linnen, R. L., Holtz, F., 1996, The combined effects of fO₂ melt composition on SnO₂ solubility tin diffusivity in haplogranitic melts. *Geochimica et Cosmochimica Acta*, v. 60(24), p. 4965-4976.

Read, H.H., 1949, A contemplation of time in Plutonism. *Quarterly Journal of the Geological Society*, v. 105, p. 101-156, doi:<https://doi.org/10.1144/GSL.JGS.1949.105.01-04.06>.

Restrepo, J.J., Toussaint, J.F., 1988, Terranes continental accretion in the Colombian es: Episodes, v. 11, p.189–193.

Restrepo, J.J., Ordóñez- Carmona, O., Armstrong, R., Pimentel, M.M., 2011, Triassic metamorphism in the northern part of the Tahamí Terrane of the central cordillera of Colombia. *J.South Am. Earth Sci*, v. 32, p.497-507.

Restrepo-Pace, P.A., Ruiz, J., Gehrels, G., Cosca, M. 1997, Geochronology Nd isotopic data of Grenville age rocks in the Colombian es: new constraints for Late Proterozoic- Early Paleozoic paleocontinental reconstructions of the Americas. *Earth Planet. Sci*, v. 150, p. 427-441.

Rochette, P., 1987, Magnetic susceptibility of the rock matrix related to magnetic fabric studies. *J. Struct.Geol*, v. 9, p. 1015-1020.

Rodríguez, G., Zapata, G., Arango, M.I., Bermúdez, J. G., 2017, Caracterización petrográfica, geoquímica y geocronología de las rocas granitoides pérmicas al occidente de La Plata y Pacaraní, Huila, Valle Superior del Magdalena, Colombia. *Bol.Geol*, v. 39, p.41-68.

Rodríguez–García, G., Correa–martínez, A. M., Zapata–García, G., Arango–Mejía, M. I., Obo–Erazo, G., Zapata–Villada, J. P., Bermúdez, J. G., 2020, Diverse Jurassic Magmatic Arcs of the Colombian es: Constraints from Petrography, Geochronology, Geochemistry. *The Geology of Colombia*, v. 2, p. 117-159.

Rudnick,R.L.,1995, Making Continental Crust. *Rev. Nature*, v. 378, p. 571-578.

Rueda-Gutiérrez, J.B., 2019, Aportes al conocimiento del Magmatismo de la Cordillera Central de Colombia en su Flanco Oriental: Área geotérmica de San Diego, Samaná, Caldas. *Revista Boletín de Geología*, v. 41, p. 45-70, doi:10.18273/revbol.v41n2-2019003.

Rudnick, R. L., Gao, S., 2003, Composition of the continental crust. *The crust*, v. 3, p. 1-64.

Sánchez, M. M., Cruz, A. D. J. G., Toro, L. M., 2008, Proveniencia del material clástico del Complejo Quebradagre y su relación con los complejos estructurales adyacentes. *Boletín de Ciencias de la Tierra*, v. 22, p. 27-38.

Sarmiento- Rojas, L.F., Van Wess, J.D., Cloetingh, S., 2006, Mesozoic transtensional basin history of the Eastern Cordillera, Colombian es: inferences from tectonic models. *J. South Am. Earth Sci.*, v. 21, p. 383-411.

Silva, S., Kay, S.M., 2018, Turning up the Heat: High-Flux Magmatism in the Central es. *Elements*, v. 14, no. 4, p. 245–250, [doi: https://doi.org/10.2138/gselements.14.4.245](https://doi.org/10.2138/gselements.14.4.245).

Spikings, R.A., Cochrane, R., Villagomez, D., Van der Lelij,R., Vallejo,C., Winkler, W., Beate, B., 2015, The geological history of northwestern south America: from Pangea to the early collision of the Caribbean large igneous province. *Gondwana Res.* 27, 95-139.

Stern, R.J., 2002. Subduction Zones. *Rev. Geophysics*, p. 1012,[doi:10.1029/2001RG000108](https://doi.org/10.1029/2001RG000108).

Spikings, R.A., Cochrane, R., Vallejo,C., Villagomez, D., Van der Lelij,R., Paul,A., Winkler, W., 2019, Latest Triassic to Early Cretaceous tectonics of the Northern es: Geochronology, geochemistry, isotopic tracing, thermochronology. *ean Tectonics*. Elsevier, p. 173-2016, doi.org/10.1016/B978-0-12-816009-1.00009-5.

Sun, S. S., McDonough, W. F.,1989, Chemical isotopic systematics of oceanic basalts: implications for mantle composition processes. Geological Society, London, Special Publications, v. 42, no. 1, p. 313-345.

Takagi, T., 2004, Origin of Magnetite- and Ilmenite- series granitic rocks in the Japan arc. *American Journal of Science*, p. 304, [doi: 10.2475/ajs.304.2.169](https://doi.org/10.2475/ajs.304.2.169).

Tarling, D., Hrouda, F., 1993, Magnetic anisotropy of rocks. Springer Science Business Media.

Taylor, S. R., McLennan, S. M.,1985, The continental crust: its composition evolution.

Taylor, S. R., McLennan, S. M., 1995, The geochemical evolution of the continental crust. *Reviews of geophysics*, v. 33, no. 2, p. 241-265.

Toussaint, J.F., Restrepo, J.J.,1994, The Colombian es during cretaceous times. In: Salfity, J.A, *Cretaceous Tectonics of the es*, p. 61-100.

Van der Lelij, R., Spikings, R., Ulianov, A., Chiaradia, M., Mora, A., 2016, Paleozoic to Early Jurrassic history of the northwestern corner of Gondwana, implications for the evolution of the Iapetus, Rheic Pacific Oceans. *Gondwana Res* v. 31, p. 271-294.

Vásquez, M., Altenberger, U., Romer, L.R., Sudo, M., Moreno-Murillo, J.M., 2010, Magmatic evolution of the Andean Eastern Cordillera of Colombia during the Cretaceous: Influence of previous tectonic processes: *Journal of South American Earth Sciences*, v. 29, no. 2, p. 171–186, [doi:10.1016/j.jsames.2009.02.003](https://doi.org/10.1016/j.jsames.2009.02.003).

Vásquez, M., Altenberger, U., 2005, Mid-Cretaceous extension-related magmatism in the eastern Colombian Andes: *Journal of South American Earth Sciences*, v. 20, no. 3, p. 193–210, doi:10.1016/j.jsames.2005.05.010.

Villagómez, D., Spikings, R., Magna, T., Kammer, A., Winkler, W., Beltrán, A., 2011, Geochronology, geochemistry tectonic evolution of the Western Central cordilleras of Colombia. *Lithos*. Elsevier, p. 875-896, doi:10.1016/j.lithos.2011.05.003.

Villagómez, D., Spikings, R., 2013, Thermochronology tectonics of the Central Western Cordilleras of Colombia: Early Cretaceous–Tertiary evolution of the Northern es: *Lithos*, v. 160–161, p. 228–249, doi: 10.1016/j.lithos.2012.12.008.

Villaseca, C., Ruiz-Martínez, V. C., Pérez-Soba, C., 2017, Magnetic susceptibility of Variscan granite-types of the Spanish Central System the redox state of magma. *Geologica Acta: an international earth science journal*, v. 15, no. 4, p. 379-394.

Vinasco, C.V., Cordani, U., González, H., Weber, M., Peláez, C., 2006, Geochronological, isotopic, geochemical data from Permo-Triassic granitic gneisses granitoids of the Colombian Central es. *Journal of South American Earth Sciences*, v. 21, p. 355–371.

Wedepohl, K. H., 1995, The composition of the continental crust. *Geochimica et cosmochimica Acta*, v. 59, no. 7, p. 1217-1232.

White, W.M., Klein, E.M., 2014, Composition of the oceanic crust. In: Holl HD, Turekian KK (eds) *Treatise on geochemistry*, 2nd edn. Elsevier, Oxford, p. 457–496. <https://doi.org/10.1016/B978-0-08-095975-7.00315-6>.

Williams, G., Powell, C., Cooper, M., 1989, *Geometry and Kinematics of Inversion Tectonics*. Geological Society, London, Special Publications, v. 44, p. 3-15, doi: 10.1144/GSL.SP.1989.044.01.02.

Zapata, G., Rodríguez, G., Arango- Mejía, M. I., 2017, Petrografía, geoquímica y geocronología de rocas metamórficas aflorantes en San Francisco Putumayo y la vía Palermo-San Luis asociadas a los complejos La Cocha- Río Téllez y Aleluya. *Bol. Cienc. Tierra*, v. 411, p. 47-64.